Quantum Sensors Assisted by Spontaneous Symmetry Breaking for Detecting Very Small Forces

Peter A. Ivanov,[1] Kilian Singer,[2] Nikolay V. Vitanov,[1] and Diego Porras[3]

[1]*Department of Physics, Sofia University, James Bourchier 5 Boulevard, 1164 Sofia, Bulgaria*
[2]*QUANTUM, Institut für Physik, Universität Mainz, D-55128 Mainz, Germany*
[3]*Department of Physics and Astronomy, University of Sussex,*
Falmer, Brighton BN1 9QH, United Kingdom

We propose a quantum-sensing scheme for measuring weak forces based on a symmetry-breaking adiabatic transition in the quantum Rabi model. We show that the system described by the Rabi Hamiltonian can serve as a sensor for extremely weak forces with sensitivity beyond the yoctonewton (yN) per $\sqrt{\text{Hz}}$ range. We propose an implementation of this sensing protocol using a single trapped ion. A major advantage of our scheme is that the force detection is performed by projective measurement of the population of the spin states at the end of the transition, instead of the far slower phonon number measurement used hitherto.

I. INTRODUCTION

Using nanoscale mechanical oscillators as detectors of extremely weak forces has attracted considerable experimental interest [1]. Such systems allow us to measure forces with sensitivity below the attonewton (aN) range which is beneficial for a broad range of applications. For example, a force detector with a nanomechanical oscillator coupled to a microwave cavity can reach sensitivity below 1 aN (10^{-18} N) per $\sqrt{\text{Hz}}$ [2]. Other sensors use mechanical oscillators made of carbon nanotubes for force detection with sensitivity in the zN (10^{-21} N) per $\sqrt{\text{Hz}}$ range [3]. Recently, the detection of ultraweak forces as small as 5 yN (10^{-24} N) was experimentally demonstrated using injection-locked ions [4]. Force measurement in an ensemble of ions in a Penning trap uses the Doppler velocimetry technique to detect force with sensitivity of 170 yN/$\sqrt{\text{Hz}}$ [5]. Another approach uses high-precision ion position determination to measure light pressure forces [6]. In all cases, the force sensing based on mechanical oscillators is carried out by converting the force into a displacement that is measured by electrical or optical means.

In this work, we introduce a different sensing protocol, which uses a system described by the quantum Rabi (QR) model as a probe that is sensitive to extremely weak forces. The QR model consists of a single bosonic mode and an effective spin system which interact via dipolar coupling. We show that the effect of symmetry breaking of the underlying parity symmetry in the QR model due to the presence of external perturbation can be used in an efficient way for detection of classical oscillating forces. Our scheme relies on the adiabatic evolution of the ground state of the QR model into the Schrödinger cat state, where the relevant force information is mapped in the respective probability amplitudes. The force sensing is performed simply by measuring the spin populations. Therefore, our protocol, which demands a single population measurement, is considerably faster than previous protocols based on the detection of the motional degree of freedom via Rabi oscillations.

We consider a particular implementation of our sensing scheme using a coherently manipulated single trapped ion. The driving parameters of the QR model can be controlled and tuned by the laser detuning and intensity [7,8]. The scheme, however, can be realized with various quantum-optical systems such as nitrogen-vacancy centers in diamond and superconducting qubits inside a microwave cavity [9–11]. We show that with the current ion trap technologies, force sensitivity below 1 yN/$\sqrt{\text{Hz}}$ can be achieved. In addition, we show that our method can be applied for detection of spin-dependent forces which are created in magnetic-field gradients or Stark-shift gradients. Hence, our method can be used for studying magnetic dipole moments of atomic or molecular ions [4,12].

II. ADIABATIC QUANTUM METROLOGY USING THE QUANTUM RABI MODEL

Our system consists of a two-level atom with states $|\uparrow\rangle$ and $|\downarrow\rangle$ coupled to a single bosonic mode described by the quantum Rabi model,

$$\hat{H}_R = \hbar\omega\hat{a}^\dagger\hat{a} + \frac{\hbar\Omega_y(t)}{2}\sigma_y + \hbar g\sigma_x(\hat{a}^\dagger + \hat{a}). \quad (1)$$

Here, $\hat{a}^\dagger$ and $\hat{a}$ are the creation and annihilation operators of bosonic excitation with frequency ω, and σ_β ($\beta = x, y, z$) are the respective Pauli matrices. The time-dependent Rabi frequency of the transverse field is given by $\Omega_y(t)$, and g is

the spin-boson coupling. Recently, it was shown that the Rabi model permits exact integrability [13].

The quantum Rabi Hamiltonian (1) possesses a discrete symmetry revealed by the parity transformation $\hat{a} \rightarrow -\hat{a}$, $\sigma_y \rightarrow \sigma_y$, and $\sigma_x \rightarrow -\sigma_x$. In the following, we consider the QR model in the regime $g \simeq \omega$ and study the effect of a small perturbation term $\hat{H}_{\text{pert}}$, which breaks the underlying parity symmetry of the model. The total Hamiltonian including the perturbation term becomes

$$\hat{H} = \hat{H}_R + \hat{H}_{\text{pert}}. \tag{2}$$

As we will see, the symmetry-breaking process allows us to estimate the perturbation term very accurately.

The measurement protocol for $\hat{H}_{\text{pert}}$ starts by preparing the system in the ground state of the unperturbed Hamiltonian $\hat{H}_R$ in the limit $\Omega_y(0) \gg g$, $4g^2/\omega$ such that $|\psi_g(0)\rangle = |-\rangle_y|0\rangle$ where $|-\rangle_y = (|\uparrow\rangle - i|\downarrow\rangle)/\sqrt{2}$, and $|n\rangle$ is the Fock state of the bosonic mode with occupation number n. Then we adiabatically decrease the transverse field $\Omega_y(t)$ in time such that the system evolves into the Schrödinger cat state

$$|\psi_g(t)\rangle = c_+(t)|\psi_+\rangle + c_-(t)|\psi_-\rangle, \tag{3}$$

where $c_\pm(t)$ are the respective probability amplitudes. Here, $|\psi_+\rangle = |+\rangle_x|\alpha\rangle$ and $|\psi_-\rangle = |-\rangle_x|-\alpha\rangle$ form the ground-state multiplet with $|\pm\rangle_x = (|\uparrow\rangle \pm |\downarrow\rangle)/\sqrt{2}$, and $|\alpha\rangle$ stands for a coherent state with amplitude $\alpha = -g/\omega$. State (3) implies that for $\hat{H}_{\text{pert}} = 0$, the parity symmetry is preserved by creating an entangled state with equal probabilities, $c_\pm = \pm 1/\sqrt{2}$. The effect of the perturbation is to break the parity symmetry of $\hat{H}_R$ by creating a ground-state wave function (3) with unequal probability amplitudes, $|c_+|^2 \neq |c_-|^2$. By measuring the respective probabilities at the end of the process, one can estimate the unknown perturbation.

In order to describe the creation of the symmetry-broken ground state, we represent the Hamiltonian (2) within the ground-state multiplet. Assuming that the parity-breaking perturbation does not couple different states in the ground-state manifold as in the case of force, we obtain an effective two-level problem with the Hamiltonian [14]

$$H_{\text{eff}} = \begin{bmatrix} \langle\psi_+|\hat{H}_{\text{pert}}|\psi_+\rangle & \hbar\Delta_{\text{gap}}/2 \\ \hbar\Delta_{\text{gap}}/2 & \langle\psi_-|\hat{H}_{\text{pert}}|\psi_-\rangle \end{bmatrix}. \tag{4}$$

Here, Δ_{gap} is the energy gap of the ground-state multiplet $\Delta_{\text{gap}} = \Omega_y e^{-2(g/\omega)^2}$ which can be estimated by calculating the matrix elements of σ_y in quasidegenerate ground-state subspace, which is valid even in the regime $g > \omega$ [see Fig. 1(a)]. Hereafter, we assume an exponential decay of
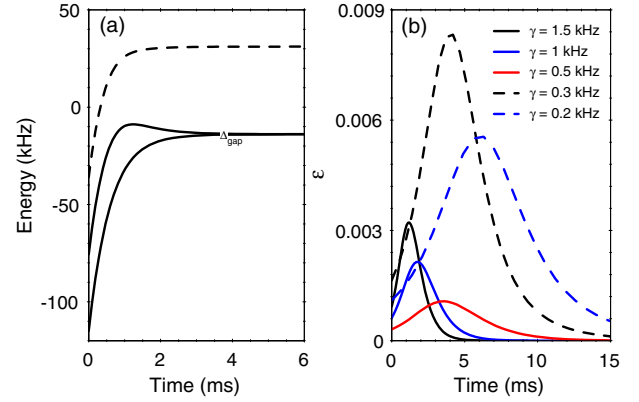

FIG. 1. (a) Low-energy spectrum of the quantum Rabi model as a function of time t. The two lowest-lying states are separated by energy splitting Δ_{gap}. At the initial moment $t = 0$, the system is prepared in the ground state with $\Omega_y(0) \gg g$ and then it evolves into the Schrödinger cat state (3). The energy difference between the third excited energy (dashed line) and the ground-state energy is Δ_{GE}. We assume $\gamma = 1.5$ kHz, $g = 25$ kHz, $\omega = 45$ kHz, and $\Omega_y(0) = 225$ kHz. (b) Adiabatic parameter ϵ versus time t for $g = 25$ kHz and $\omega = 45$ kHz (solid lines), $\omega = 20$ kHz (dashed lines), and various values of γ.

the transverse field $\Omega_y(t) = \Omega_y(0)e^{-\gamma t}$ with a characteristic slope γ which implies that $\Delta_{\text{gap}} \sim e^{-\gamma t}$. The latter energy gap reduces the two-state problem represented by the effective Hamiltonian (4) to the Demkov model [15,16]. The adiabaticity of the process is characterized by the condition $\epsilon = |\langle\psi_g|d/dt|\psi_e\rangle/\Delta_{\text{GE}}| \ll 1$, which requires the coupling between the ground state $|\psi_g\rangle$ to the first excited state $|\psi_e\rangle$ to be much smaller that the energy gap between them Δ_{GE} at any instant of time. Note that because of the absence of fast driven oscillations in our system, the adiabatic condition $\epsilon \ll 1$ is sufficient [17–19]. In Fig. 1(b), we show the adiabatic parameter ϵ during the creation of the Schrödinger cat state (3) for various γ. We observe that the nonadiabatic transitions become stronger for $g \geq \omega$ compared to the regime $g < \omega$. On the other hand, the adiabaticity is fulfilled for lower γ.

At the final stage, the externally applied perturbation is detected by measuring the expectation value of σ_x. An analytical expression for the measured signal can be derived by solving the quantum evolution of a two-level system with the Hamiltonian (4) for the specific time dependence of $\Omega_y(t)$.

III. SENSING WEAK FORCES AND DISPLACEMENTS

In the following, we consider a harmonic oscillator represented by a single trapped ion with mass m confined in a Paul trap with an axial trap frequency ω_z. We assume that the effective spin system of the ion is implemented by two metastable atomic levels $|\uparrow\rangle$ and $|\downarrow\rangle$ with a transition

frequency ω_0. We describe the small axial vibrations of the ion by the following motional Hamiltonian

$$\hat{H}_m = \hbar\omega\hat{a}^\dagger\hat{a}, \qquad \hat{z} = z_0(\hat{a}^\dagger + \hat{a}), \qquad (5)$$

where $\hat{a}^\dagger$ and $\hat{a}$ are the respective phonon creation and annihilation operators, and $z_0 = \sqrt{\hbar/2m\omega_z}$ is the spread of the oscillator ground-state wave function [8].

A. Electric-field sensing

The ability to control the motional and internal states with high accuracy makes the trapped ions a formidable experimental tool for electric-field sensing [5,6,20,21]. In contrast to the conventional methods which rely only on the detection of the motional degrees of freedom [21–26], here the relevant information is transferred directly into the spin degrees of freedom due to the use of the symmetry-breaking adiabatic transition. In the following, we assume that a classical oscillating force $F(t) = F_d\cos(\omega_d t)$ with an amplitude F_d—the parameter we wish to estimate—and frequency $\omega_d = \omega_z - \omega$ shifted from the axial trap frequency ω_z by a small detuning ω ($\omega_z \gg \omega$) is applied to the ion. The action of the force is to displace the motional amplitude of the ion's vibrational oscillator described by

$$\hat{H}_F = F(t)\hat{z}(t) = \frac{z_0 F_d}{2}(\hat{a}^\dagger e^{i\omega t} + \hat{a}e^{-i\omega t}), \qquad (6)$$

where we neglect the fast-rotating terms. Note that in terms of motion and position, the following discussion is restricted to 1D. In order to implement the spin-boson term in the quantum Rabi Hamiltonian (2), we assume that the ion is simultaneously addressed by bichromatic laser fields in a Raman configuration with a wave-vector difference $\Delta\vec{k}$ along the z direction, which induces a transition between the spin states via an auxiliary excited state. By setting the laser frequency beat notes $\omega_r = \omega_0 - \omega_z + \omega$ and $\omega_b = \omega_0 + \omega_z - \omega$ close to the red and blue sideband transitions of the vibrational mode ω_z, the resulting Hamiltonian in the Lamb-Dicke limit ($\eta \ll 1$) becomes [8,27]

$$\hat{H}_{SB} = \hbar g\sigma_x(\hat{a}^\dagger e^{i\omega t} + \hat{a}e^{-i\omega t}), \qquad (7)$$

where $g = \Omega\eta$ is the spin-phonon coupling with Ω being the two-photon Rabi frequency, and η stands for the Lamb-Dicke parameter. The transverse field in Eq. (2) can be created by driving the resonant carrier transition between the internal spin states using a microwave or radio-frequency field, which yields

$$\hat{H}_y(t) = \frac{\hbar\Omega_y(t)}{2}(e^{i\phi}|\uparrow\rangle\langle\downarrow| + \text{H.c.}) = \frac{\hbar\Omega_y(t)}{2}\sigma_y. \qquad (8)$$

Here, $\Omega_y(t)$ is the time-dependent Rabi frequency, and we set the driving phase to $\phi = -\pi/2$. In the interaction picture

rotating at the frequency ω, the total Hamiltonian $\hat{H} = \hat{H}_{SB} + \hat{H}_y + \hat{H}_F$ is given by Eq. (2) where the symmetry-breaking term is

$$\hat{H}_{pert} = \frac{z_0 F_d}{2}(\hat{a}^\dagger + \hat{a}). \qquad (9)$$

The force-sensing protocol starts by initialization of the spins along the y direction and laser cooling of the single-ion vibrational mode to the motional ground state. Subsequently, the transverse field exponentially decays as $\Omega_y(t) = \Omega_y(0)e^{-\gamma t}$, which drives the system adiabatically into the superposition state $|\psi_g(t)\rangle = c_+(t)|\psi_+\rangle + c_-(t)|\psi_-\rangle$. Here, $c_\pm(t)$ are the respective probability amplitudes which are solutions of the time-dependent Schrödinger equation with the Hamiltonian (4) (see the Appendix for details). In our scheme, the detection of the force is performed either by measuring the expectation value of σ_x or by measuring the position quadrature $\hat{Z} = \hat{a}^\dagger + \hat{a}$ of the bosonic field.

For vanishing force ($F_d = 0$), the parity symmetry is restored by creating an entangled ground state that is an equal superposition of states $|\psi_\pm\rangle$, which leads to $\langle\sigma_x(t_f)\rangle = 0$ and $\langle\hat{Z}(t_f)\rangle = 0$. For $F_d \neq 0$, the parity symmetry of $\hat{H}_D$ is broken, which allows us to estimate F_d by measuring σ_x or $\hat{Z}$. In Fig. 2(a), the time evolution of the expectation value of σ_x in the presence of the symmetry-breaking term (9) is shown. At the interaction time $t_f \gg \gamma$,
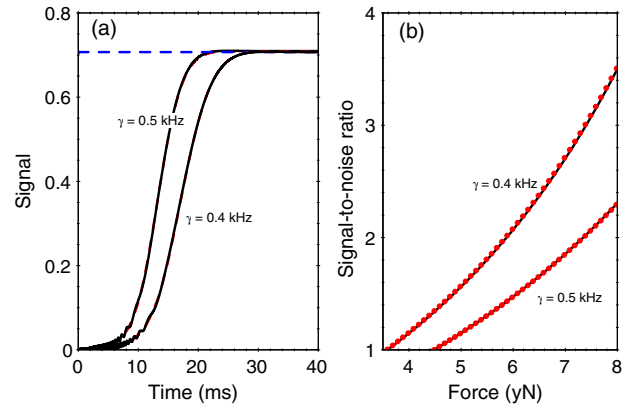

FIG. 2. (a) Time evolution of the expectation value of σ_x (solid lines) for minimal detectable force (11) and different γ. The dashed curves correspond to the solution with the effective Hamiltonian (A1), and they are nearly indistinguishable with the exact solution. At $t_f \gg \gamma^{-1}$, the signal tends to the asymptotic formula (10a) (blue dashed line). We assume a single ^{24}Mg$^+$ trapped ion with an axial trap frequency $\omega_z = 6.3$ MHz. The other parameters are set to $g = 25$ kHz, $\omega = 110$ kHz, $\Omega_y(0) = 225$ kHz. (b) Signal-to-noise (SNR) ratio versus F_d. We compare the numerical solution of the time-dependent Schrödinger equation with the Hamiltonian (2) (dots) with the asymptotic expression given by SNR = $\sinh[\pi g z_0 F_d/(\hbar\gamma\omega)]$ (solid lines).

the signal and its variance are described by (see the Appendix)

$$\langle \sigma_x(t_f) \rangle = \tanh\left(\frac{\pi g z_0 F_d}{\hbar \gamma \omega}\right), \tag{10a}$$

$$\langle \Delta^2 \sigma_x(t_f) \rangle = 1 - \langle \sigma_x(t_f) \rangle^2. \tag{10b}$$

Note that compared to other schemes, here the sign of the force in Eq. (9) is fully preserved due to the tanh dependence of the signal. The corresponding signal-to-noise ratio SNR $= \langle \sigma_x(t_f) \rangle / \langle \Delta^2 \sigma_x(t_f) \rangle^{1/2}$ is shown in Fig. 2(b). The minimum detectable force is determined by the condition that the signal-to-noise ratio is equal to 1, which gives

$$F_d^{\min} = \frac{\hbar \gamma \omega}{\pi g z_0} \sinh^{-1}(1). \tag{11}$$

We compare our minimal detectable force with those using a simple harmonic oscillator as a force sensor. In that case, the signal-to-noise ratio of 1 gives $F_{\rm HO}^{\min} = 2\hbar / z_0 t$ [21]. Our scheme allows us to overcome this limit by tuning the ratio ω / g. For example, assuming $g = 44$ kHz, $\omega = 30$ kHz, $\gamma = 0.2$ kHz, and evolution time of $t_f = 48$ ms, we verify numerically that $F_d^{\min} \approx 0.92 F_{\rm HO}^{\min}$. The standard quantum limit derived by the time-energy uncertainty, however, gives $F_{\rm HO}^{\min} / 2$ [25,28]. This limit can be approached by further decreasing ω / g. However, we note that decreasing ω / g cannot increase the accuracy of the detection method indefinitely. Very low values of ω lead to longer evolution times required to stay within the adiabatic regime.

The sensitivity of the force measurement is defined as $\eta_{\rm force} = F_d^{\min} / \sqrt{\nu}$, where $\nu = T/\tau$ is the repetition number with T being the total experimental time. The time τ includes the evolution time as well as the preparation and measurement times. Because our scheme relies on the projective measurement of the spin populations at the end of the adiabatic transition, we have $\tau \approx t_f$. The sensitivity characterizes the minimal force difference, which can be discriminated within a total experimental time of 1 s. In Fig. 3, we show the sensitivity as a function of the slope γ for various values of ω. Lowering γ implies a longer interaction time t_f and, thus, better sensitivity. Using the parameters in Fig. 3 for $\omega = 45$ kHz and interaction time $t_f = 30$ ms, we estimate force sensitivity of about 0.3 yN$/\sqrt{\rm Hz}$. Further increasing of the sensitivity to 0.16 yN$/\sqrt{\rm Hz}$ can be achieved with the interaction time of $t_f = 100$ ms.

Alternatively, the force estimation can be carried out by measuring the expectation value of the position quadrature $\langle \hat{Z}(t_f) \rangle$. We find
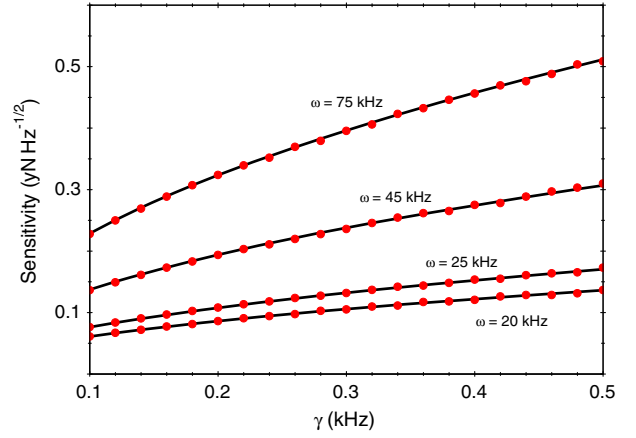

FIG. 3. The sensitivity $\eta_{\rm force} \sqrt{T}$ versus the slope γ for various values of ω. We assume a single ^{24}Mg$^+$ ion with an axial trap frequency $\omega_z = 6.3$ MHz. The interaction time is set to $t_f = 14\gamma^{-1}$. The other parameters are $g = 25$ kHz, $\Omega_y(0) = 225$ kHz. The exact solution with Hamiltonian (2) (dots) is compared with the analytical expression $\eta_{\rm force} \sqrt{T} = \sqrt{t_f} F_d^{\min}$ (solid line) where $F_d^{\min}$ is given by Eq. (11).

$$\langle \hat{Z}(t_f) \rangle = -2\frac{g}{\omega} \tanh\left(\frac{\pi g z_0 F_d}{\hbar \gamma \omega}\right),$$

$$\langle \Delta^2 \hat{Z}(t_f) \rangle = 1 + 4\frac{g^2}{\omega^2} - \langle \hat{Z}(t_f) \rangle^2. \tag{12}$$

Using Eq. (12), we obtain that for $\omega > 2g$ the uncertainty of the position quadrature is higher than the measured signal (SNR < 1). At $\omega = 2g$ and in the limit $F_d \gg 2\gamma\hbar/(\pi z_0)$, the SNR tends asymptotically to one from below, and, thus, no measurement is possible, whereas for $\omega < 2g$, the force estimation is bounded by

$$F_d^{\min} = \frac{\hbar \gamma \omega}{\pi g z_0} \tanh^{-1}\sqrt{\frac{1}{2} + \frac{\omega^2}{8g^2}}. \tag{13}$$

Comparing Eqs. (11) and (13), we conclude that the signal of σ_x provides better sensitivity. Moveover, the direct detection of the quantum motional state requires additional operations after the sensing protocol. Such operations include the observation of the time evolution of the spin states under the influence of Jaynes-Cummings-type interaction [29]. Our scheme avoids those additional operations since it relies on simple fluorescence measurements of the spin states, and, thus, there is no requirement of additional time-evolution steps after the adiabatic process. This simplifies the experimental measurement procedure and can lead to the reduction of the total experimental time.

B. Effect of motional heating

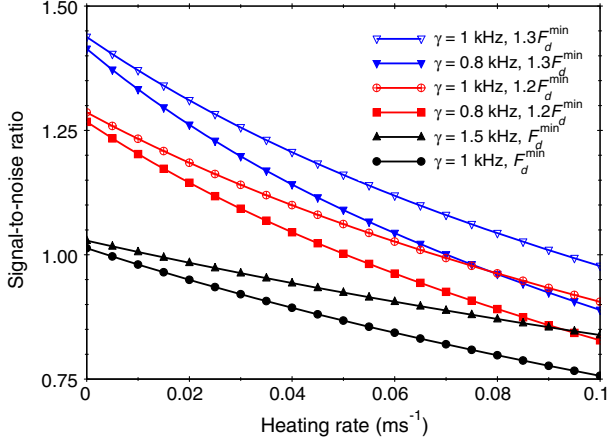The main source of decoherence which limits the force estimation in our scheme is caused by the motional heating.

FIG. 4. Signal-to-noise ratio versus the heating rate for various values of γ and F_d. We integrate numerically the master equation (14) with the Hamiltonian (2). The other parameters are set to $g = 25$ kHz, $\omega = 150$ kHz, and $\Omega_y(0) = 225$ kHz.

In order to account for the effect of the motional heating in the sensing protocol, we numerically integrate the master equation

$$\frac{d\hat{\rho}}{dt} = -\frac{i}{\hbar}[\hat{H}, \hat{\rho}] + \frac{\gamma_{\text{dec}}}{2}(\bar{n} + 1)(2\hat{a}\,\hat{\rho}\,\hat{a}^\dagger - \hat{a}^\dagger\hat{a}\,\hat{\rho} - \hat{\rho}\hat{a}^\dagger\hat{a})$$
$$+ \frac{\gamma_{\text{dec}}}{2}\bar{n}(2\hat{a}^\dagger\hat{\rho}\,\hat{a} - \hat{a}\hat{a}^\dagger\hat{\rho} - \hat{\rho}\,\hat{a}\,\hat{a}^\dagger). \tag{14}$$

Here, γ_{dec} is the system decay rate, and $\bar{n}$ is the average number of quanta in the reservoir. In the limit $\bar{n} \gg 1$, the motional heating is characterized by the time $t_{\text{dec}} = 1/(\bar{n}\gamma_{\text{dec}})$ and the heating rate is $\langle\dot{n}\rangle = 1/t_{\text{dec}}$. In Fig. 4, we show the signal-to-noise ratio for σ_x as a function of $\langle\dot{n}\rangle$. By increasing the heating rate, the corresponding signal-to-noise ratio decreases with stronger damping for lower γ and ω. Note that for small γ, the effect of the motional heating is stronger, since the evolution time $t \sim \gamma^{-1}$ is longer. Using the parameters presented in Fig. 4, we estimate sensitivity of 1.9 yN/$\sqrt{\text{Hz}}$ within the interaction time $t_f = 14$ ms and heating rate of approximately 0.1 ms^{-1}, which corresponds to typical heating rates in linear ion Paul traps. For a cryogenic ion trap with heating rate of order of $\langle\dot{n}\rangle = 0.01$ ms^{-1} [30], the force sensitivity will be approximately of 0.7 yN/$\sqrt{\text{Hz}}$ for $\omega = 75$ kHz and $\gamma = 0.8$ kHz.

C. Effect of the ac Stark shift

The particular Raman configuration that we use to implement the QR model gives rise to an additional ac Stark-shift term $\hat{H}' = \chi\sigma_z$ in Eq. (2) where $\chi = \chi_\uparrow - \chi_\downarrow$ is the light shift of the atomic levels caused by the optical fields. The effect of $\hat{H}'$ is to couple the states $|\psi_\pm\rangle$, and, thus, it leads to lifting of the degeneracy of the ground-state multiplet. Compensation of the ac Stark shift can be achieved, for example, by proper tuning of the Raman

beam differences or by adjustment of the polarization of the corresponding laser beams [27,31]. However, any uncompensated ac Stark shift can induce dephasing of the atomic levels due to the intensity fluctuations of the Raman laser beams, which will limit the force sensitivity. In order to study its effect, we solve numerically the master equation for the Hamiltonian (2) including the dissipative term $\hat{L}(\hat{\rho}) = \frac{1}{2}\Gamma(\sigma_z\hat{\rho}\sigma_z - \hat{\rho})$ where $\Gamma = 1/\tau_{\text{dec}}$ stands for the constant dephasing rate, and τ_{dec} is the decoherence time. The result shows that the corresponding SNR decays as a function of Γ with stronger damping for lower γ. For example, assuming $\tau_{\text{dec}} = 50$ ms and $g = 25$ kHz, $\omega = 120$ kHz, $\gamma = 2$ kHz, we estimate force sensitivity to approximately 1.5 yN/$\sqrt{\text{Hz}}$ within the interaction time of $t_f = 5$ ms.

We note that, alternatively, the QR model can be implemented by using magnetic sensitive states driven by radio-frequency fields and a static-magnetic-field gradient. Then, by using microwave dressing fields, the effect of the undesired σ_z term can be highly suppressed as was experimentally demonstrated [32,33].

IV. SENSING OF SPIN-DEPENDENT FORCES

Here we introduce a measurement protocol that can be used for sensing of spin-dependent forces. The origin of such forces can be due to (i) spatially dependent Zeeman shift experiences by spins in a magnetic-field gradient [34] or (ii) spatially dependent Stark shifts experienced by atoms in an intensity-field gradient, which give rise to an optical dipole force [35]. Consider the case of an oscillating magnetic-field gradient along the trap axis. Consider also an ion chain with two ions where the internal states of the first ion are formed by the magnetic-insensitive clock states $|s\rangle_{\text{clock}}$ with $s = \uparrow, \downarrow$. These clock states are used to implement the quantum Rabi Hamiltonian (1) taking $\sigma_x = (|\uparrow\rangle_{\text{clock}}\langle\downarrow| + \text{H.c.})$ and $\sigma_y = i(|\downarrow\rangle_{\text{clock}}\langle\uparrow| - \text{H.c.})$ with the same method as described above. The auxiliary ion (not necessarily the same atomic species) is prepared in one of its magnetic-sensitive states $|\text{aux}\rangle$. The external oscillating magnetic-field gradient $\vec{B}(t) = \cos(\omega t)B_0 z\vec{e}_z$ will create a coupling between the auxiliary ion states and the collective vibrational modes. Assuming that the oscillating frequency is close to the center-of-mass vibrational mode $\omega = \omega_{\text{c.m.}} - \omega$ and neglecting the fast oscillating terms, we arrive at

$$\langle\text{aux}|\hat{H}_{\text{pert}}|\text{aux}\rangle = \frac{z_{\text{c.m.}}F_z}{\sqrt{2}}(\hat{a}^\dagger + \hat{a}), \tag{15}$$

where $z_{\text{c.m.}} = \sqrt{\hbar/2m\omega_{\text{c.m.}}}$. Here, $F_z = g_J\mu_B B_0/2$ is the force acting on the magnetic moment $\mu_z^{\text{aux}} = (g_J\mu_B/2)|\text{aux}\rangle\langle\text{aux}|$ of the auxiliary ions where g_J is the Lande g factor, and μ_B is the Bohr magneton. The induced force on the clock ion can be used for studying, e.g., the

magnetic moment of the auxiliary atomic or molecular ions trapped together with the clock ion. Indeed, assuming magnetic dipole moment $2\mu_B$ of the auxiliary ion and magnetic-field gradient of 1 T/m, the resulting force is about 9 yN, which can be detected by measuring the spin population of the clock ions. We note that a similar technique for measuring the nuclear magnetic dipole moment is proposed in Ref. [4] using injection-locked ions.

V. CONCLUSIONS

We show that the system described by the quantum Rabi Hamiltonian can serve as a detector of extremely small forces. The underlying physical mechanism is the process of symmetry-breaking adiabatic transition due to the presence of force perturbations. Our sensing protocols can be implemented using a trapped ion, where the parameters which drive the system across the adiabatic transition are controlled by external laser or microwave fields. We show that a system of a single trapped ion can be used as a probe for electric sensing with sensitivity about and even below the 1 yN/$\sqrt{\text{Hz}}$ range. Additionally, the proposed method can be extended for sensing magnetic fields. A major advantage of our protocol is that it demands a single population measurement, thereby achieving a considerable speed-up over previous protocols using phonon number measurement via Rabi oscillations.

ACKNOWLEDGMENTS

APPENDIX: DERIVATION OF THE SIGNAL AND VARIANCE OF THE SIGNAL

In the symmetry-broken phase, the underlying dynamics of the QR Hamiltonian with the perturbation term (9) can be captured within the two-level model with the effective Hamiltonian

$$H_{\text{eff}} = \begin{bmatrix} -z_0 F_d \frac{g}{\omega} & \hbar\Delta_{\text{gap}}(t)/2 \\ \hbar\Delta_{\text{gap}}(t)/2 & z_0 F_d \frac{g}{\omega} \end{bmatrix}. \quad (A1)$$

The probability amplitudes $c_{\pm}(t)$ for the state vector $|\psi_g(t)\rangle = c_+(t)|\psi_+\rangle + c_-(t)|\psi_-\rangle$ obey the time-dependent Schrödinger equation, which turns into a system of two coupled differential equations

$$i\dot{c}_+(t) = -\frac{z_0 F_d g}{\hbar\omega} c_+(t) + \frac{\Delta_{\text{gap}}(t)}{2} c_-(t), \quad (A2a)$$

$$i\dot{c}_-(t) = \frac{z_0 F_d g}{\hbar\omega} c_-(t) + \frac{\Delta_{\text{gap}}(t)}{2} c_+(t) \quad (A2b)$$

subject to the initial conditions $c_+(t_i) = 1/\sqrt{2}$ and $c_-(t_i) = -1/\sqrt{2}$. We assume that the transverse field varies in time as $\Omega_y(t) = \Omega_y(t_i)e^{-\gamma t}$, which implies that $\Delta_{\text{gap}}(t) = \Delta_i e^{-\gamma t}$ and the two-state problem reduces to the Demkov model. The system for the probability amplitudes is decoupled by differentiating with respect to t, which yields

$$z^2 \frac{d^2 c_{\pm}}{dz^2} + \left\{ z^2 + \left(\frac{z_0 F_d g}{\hbar\gamma\omega}\right)^2 \mp i\frac{z_0 F_d g}{\hbar\gamma\omega} \right\} c_{\pm} = 0. \quad (A3)$$

Here we introduce the dimensionless time $z = xe^{-\gamma t}$ with $x = \Delta_i/2\gamma$. The solution can be written as [36]

$$c_+(z) = \sqrt{z}\{a_1 J_\nu(z) + a_2 J_{-\nu}(z)\}, \quad (A4a)$$

$$c_-(z) = \sqrt{z}\{b_1 J_{1-\nu}(z) + b_2 J_{\nu-1}(z)\}, \quad (A4b)$$

where $J_\nu(z)$ is the Bessel function of first kind with $\nu = 1/2 + iz_0 F_d g/\hbar\gamma\omega$ and $a_{1,2}$, $b_{1,2}$ are constants which are determined by the initial conditions. In the limit $t_f \gg \gamma^{-1}$ such that $J_\nu(z) \sim [1/\Gamma(1+\nu)](z/2)^\nu$ for $z \ll 1$ and using the asymptotic form $J_\nu(x) \sim \sqrt{2\pi x}\cos[x - (\pi\nu/2) - (\pi/4)]$ for $x \gg |\nu^2 - 1/2|$, we arrive at

$$|c_+(t_f)|^2 = \frac{1}{2} + \frac{1}{2}\tanh\left(\frac{\pi g z_0 F_d}{\hbar\gamma\omega}\right) \quad (A5)$$

and $|c_-(t_f)|^2 = 1 - |c_+(t_f)|^2$. The expectation value and the variance of σ_x with respect to $|\psi(t_f)\rangle$ are

$$\langle\sigma_x(t_f)\rangle = 2|c_+(t_f)|^2 - 1, \quad (A6a)$$

$$\langle\Delta^2\sigma(t_f)\rangle = 4|c_+(t_f)|^2|c_-(t_f)|^2. \quad (A6b)$$

For the measured signal of the quadrature $\hat{Z}$ and its variance, we find

$$\langle Z(t_f)\rangle = 2\alpha(2|c_+(t_f)|^2 - 1), \quad (A7a)$$

$$\langle\Delta^2 Z(t_f)\rangle = 1 + 16\alpha^2|c_+(t_f)|^2|c_-(t_f)|^2. \quad (A7b)$$

[1] H. J. Mamin and D. Rugar, Sub-attonewton force detection at millikelvin temperatures, Appl. Phys. Lett. **79**, 3358 (2001).

[2] J. D. Teufel, T. Donner, M. A. Castellanos-Beltran, J. W. Harlow, and K. W. Lehnert, Nanomechanical motion

measured with an imprecision below that at the standard quantum limit, Nat. Nanotechnol. **4,** 820 (2009).

[3] J. Moser, J. Güttinger, A. Eichler, M. J. Esplandiu, D. E. Liu, M. I. Dykman, and A. Bachtold, Ultrasensitive force detection with a nanotube mechanical resonator, Nat. Nanotechnol. **8,** 493 (2013).

[4] S. Knünz, M. Herrmann, V. Batteiger, G. Saathoff, T. W. Hänsch, K. Vahala, and Th. Udem, Injection Locking of a Trapped-Ion Phonon Laser, Phys. Rev. Lett. **105,** 013004 (2010).

[5] M. J. Biercuk, H. Uys, J. W. Britton, A. P. VanDevender, and J. J. Bollinger, Ultrasensitive detection of force and displacement using trapped ions, Nat. Nanotechnol. **5,** 646 (2010).

[6] T. F. Gloger, P. Kaufmann, D. Kaufmann, M. T. Baig, T. Collath, M. Jojanning, and C. Wunderlich, Ion trajectory analysis for micromotion minimization and the measurement of small forces, arXiv:1503.07031.

[7] D. J. Wineland, C. Monroe, W. M. Itano, D. Leibfried, B. E. King, and D. M. Meekhof, Experimental issues in coherent quantum-state manipulation of trapped atomic ions, J. Res. Natl. Inst. Stand. Technol. **103,** 259 (1998).

[8] C. Schneider, D. Porras, and T. Schaetz, Experimental quantum simulations of many-body physics with trapped ions, Rep. Prog. Phys. **75,** 024401 (2012).

[9] T. Niemczyk, F. Deppe, H. Huebl, E. P. Menzel, F. Hocke, M. J. Schwarz, J. J. Garcia-Ripoll, D. Zueco, T. Hümmer, E. Solano, A. Marx, and R. Gross, Circuit quantum electrodynamics in the ultrastrong-coupling regime, Nat. Phys. **6,** 772 (2010).

[10] D. Ballester, G. Romero, J. J. Garcia-Ripoll, F. Deppe, and E. Solano, Quantum Simulation of the Ultrastrong-Coupling Dynamics in Circuit Quantum Electrodynamics, Phys. Rev. X **2,** 021007 (2012).

[11] L. J. Zou, D. Marcos, S. Diehl, S. Putz, J. Schmiedmayer, J. Majer, and P. Rabl, Implementation of the Dicke Lattice Model in Hybrid Quantum System Arrays, Phys. Rev. Lett. **113,** 023603 (2014).

[12] H. Loh, S. Ding, R. Hablutzer, G. Maslennikov, and D. Matsukevich, Zeeman-splitting-assisted quantum-logic spectroscopy of trapped ions, Phys. Rev. A **90,** 061402(R) (2014).

[13] D. Braak, Integrability of the Rabi Model, Phys. Rev. Lett. **107,** 100401 (2011).

[14] P. A. Ivanov and D. Porras, Adiabatic quantum metrology with strongly correlated quantum optical systems, Phys. Rev. A **88,** 023803 (2013).

[15] Y. N. Demkov, Charge transfer at small resonance defects, Sov. Phys. JETP **18,** 138 (1964).

[16] N. V. Vitanov, Generalized Demkov model: Strong-coupling approximation, J. Phys. B **26,** L53 (1993).

[17] K.-P. Marzlin and B. C. Sanders, Inconsistency in the Application of the Adiabatic Theorem, Phys. Rev. Lett. **93,** 160408 (2004).

[18] M. H. S. Amin, Consistency of the Adiabatic Theorem, Phys. Rev. Lett. **102,** 220401 (2009).

[19] J. Ortigoso, Quantum adiabatic theorem in light of the Marzlin-Sanders inconsistency, Phys. Rev. A **86,** 032121 (2012).

[20] M. Harlander, M. Brownnutt, W. Hänsel, and R. Blatt, Trapped-ion probing of light-induced charging effects on dielectrics, New J. Phys. **12,** 093035 (2010).

[21] R. Maiwald, D. Leibfried, J. Britton, J. C. Bergquist, G. Leuchs, and D. J. Wineland, Stylus ion trap for enhanced access and sensing, Nat. Phys. **5,** 551 (2009).

[22] G. Binnig, C. F. Quate, and Ch. Gerber, Atomic Force Microscope, Phys. Rev. Lett. **56,** 930 (1986).

[23] C. M. Caves, K. S. Thorne, R. W. P. Drever, V. D. Sandberg, and M. Zimmermann, On the measurement of a weak classical force coupled to a quantum-mechanical oscillator. I. Issues of principle, Rev. Mod. Phys. **52,** 341 (1980).

[24] D. Rugar, R. Budakian, H. J. Mamin, and B. W. Chui, Single spin detection by magnetic resonance force microscopy, Nature (London) **430,** 329 (2004).

[25] W. J. Munro, K. Nemoto, G. J. Milburn, and S. L. Braunstein, Weak-force detection with superposed coherent states, Phys. Rev. A **66,** 023819 (2002).

[26] A. Ourjoumtsev, H. Jeong, R. Tualle-Brouri, and P. Grangier, Generation of optical "Schrödinger cats" from photon number states, Nature (London) **448,** 784 (2007).

[27] P. J. Lee, K.-A. Brickman, L. Deslauriers, P. C. Haljan, L.-M. Duan, and C. Monroe, Phase control of trapped ion quantum gates, J. Opt. B **7,** S371 (2005).

[28] J. Anandan and Y. Aharonov, Geometry of Quantum Evolution, Phys. Rev. Lett. **65,** 1697 (1990).

[29] D. M. Meekhof, C. Monroe, B. E. King, W. M. Itano, and D. J. Wineland, Generation of Nonclassical Motional States of a Trapped Atom, Phys. Rev. Lett. **76,** 1796 (1996).

[30] J. Chiaverini and J. M. Sage, Insensitivity of the rate of ion motional heating to trap-electrode material over a large temperature range, Phys. Rev. A **89,** 012318 (2014).

[31] F. Schmidt-Kaler, H. Häffner, S. Gulde, M. Riebe, G. P. T. Lancaster, T. Deuschle, C. Becher, W. Hänsel, J. Eschner, C. F. Roos, and R. Blat, How to realize a universal quantum gate with trapped ions, Appl. Phys. B **77,** 789 (2003).

[32] N. Timoney, I. Baumgart, M. Johanning, A. F. Varon, M. B. Plenio, A. Retzker, and Ch. Wunderlich, Quantum gates and memory using microwave-dressed states, Nature (London) **476,** 185 (2011).

[33] S. C. Webster, S. Weidt, K. Lake, J. J. McLoughlin, and W. K. Hensinger, Simple Manipulation of a Microwave Dressed-State Ion Qubit, Phys. Rev. Lett. **111,** 140501 (2013).

[34] F. Mintert and C. Wunderlich, Ion-Trap Quantum Logic Using Long-Wavelength Radiation, Phys. Rev. Lett. **87,** 257904 (2001).

[35] D. B. Hume, C. W. Chou, D. R. Leibrandt, M. J. Thorpe, D. J. Wineland, and T. Rosenband, Trapped-Ion State Detection through Coherent Motion, Phys. Rev. Lett. **107,** 243902 (2011).

[36] M. Abramowitz and I. A. Stegun, *Handbook of Mathematical Functions* (Dover, New York, 1964).